Intracranial Hemodynamics Is Altered by Carotid Artery Disease and After Endarterectomy

A Dynamic Magnetic Resonance Angiography Study

Bradley J. MacIntosh, PhD; Ediri Sideso, MBBS, MRCS; Manus J. Donahue, PhD; Michael A. Chappell, DPhil; Matthias Günther, PhD; Ashok Handa, FRCS; James Kennedy, MSc; Peter Jezzard, PhD

Background and Purpose—Carotid endarterectomy (CEA) has become a routine procedure to treat symptomatic carotid artery disease and reduce the risk of recurrent cerebral ischemic events. The purpose of this study was to use an arterial spin labeling dynamic magnetic resonance angiography technique to characterize intracranial hemodynamics before and after CEA.

Methods—Thirty-seven carotid artery disease patients participated in this study, of whom 24 underwent magnetic resonance imaging before and after CEA. Seventeen control subjects spanning 5 decades underwent magnetic resonance imaging to assess age-related changes. Hemodynamic metrics (that is, relative time to peak and amplitude) were calculated with a γ-variate model. Linear regression was used to relate carotid artery disease burden to downstream hemodynamics in the circle of Willis.

Results—Relative time to peak increased with age in controls ($P<0.020$). For patients, relative time to peak was positively correlated with percent stenosis ($P<0.050$), independent of age. At 1 day after CEA, the middle cerebral artery ipsilateral to the CEA showed significant dynamic magnetic resonance angiography changes: relative time to peak decreased ($P<0.017$) and the flow amplitude increased ($P<0.009$). No pre- versus post-CEA changes were significant in the contralateral middle cerebral artery or posterior segments.

Conclusions—This noninvasive, arterial spin labeling–based method produced time-resolved images that were used to characterize intracranial arterial flow associated with aging, extracranial carotid artery disease, and CEA. Results demonstrate that the technique has the sensitivity to detect hemodynamic changes after CEA. **(*Stroke*. 2011;42:979-984.)**

Key Words: endarterectomy ■ carotid stenosis ■ arterial spin labeling ■ angiography ■ dynamic ■ blood flow ■ aging

Atherosclerosis is a major risk factor for ischemic cerebrovascular events. Extracranial steno-occlusive disease influences hemodynamics and physiology in the brain.[1] Therefore, carotid endarterectomy (CEA) is a standard treatment for patients with symptomatic stenosis >70% because surgical therapy is associated with higher event-free survival compared with medical therapy.[2] However, CEA is not without risk; 1 study reported a 4.3% increase in the risk of stroke or death within 30 days of CEA.[2] Other studies report silent infarcts, evident postoperatively on diffusion-weighted images in 17% to 33% of CEA patients.[3,4] Therefore, there is merit in developing imaging techniques that can be used to assess the downstream impact of extracranial steno-occlusive disease.

Time-of-flight (TOF) magnetic resonance angiography (MRA) measures static arterial anatomy, whereas phase-contrast MRA is capable of quantitative flow information. Using TOF and phase-contrast MRA, others were able to quantify changes in vessel diameter and flow directionality in the circle of Willis after CEA.[5] Time-resolved, contrast-enhanced MRA is well established[6] and provides dynamic MRA information. In the interest of developing noninvasive, dynamic, MRA (DynAngio) techniques, this study introduces a variant on arterial spin labeling (ASL)[7,8] that allows quantification of magnetically labeled water in arterial blood with good spatial and temporal resolution.[9,10] Compared with phase-contrast MRA, this method does not involve velocity

Received July 29, 2010; accepted November 4, 2010.

From the Department of Clinical Neurology (B.J.M., M.J.D., M.A.C., P.J.), FMRIB Centre, Oxfordshire, England; Nuffield Department of Surgery (E.S., A.H.) and Acute Stroke Programme (E.S., J.K.), Nuffield Department of Clinical Medicine, John Radcliffe Hospital, University of Oxford, Oxfordshire, England; Department of Medical Biophysics (B.J.M.), University of Toronto, Toronto, Canada; and Department of Neurology (M.G.), University Hospital Mannheim, University of Heidelberg, and Mediri GmbH, Heidelberg, Germany.

The online-only Data Supplement is available at http://stroke.ahajournals.org/content/full/stroke.110.590786/DC1.

Correspondence to Bradley MacIntosh, PhD, Sunnybrook Health Sciences Centre, A453, 2075 Bayview Avenue, Toronto, ON, Canada, M4N 3M5. E-mail bmac@sri.utoronto.ca

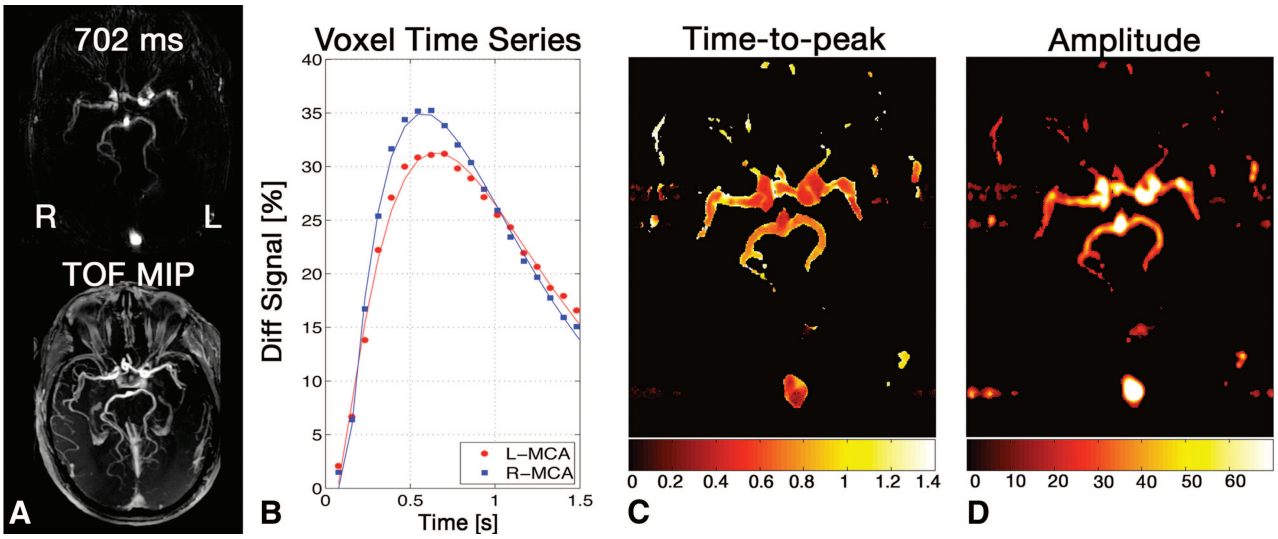

Figure 1. Dynamic intracranial ASL angiography data for an 82-year-old woman with 60% stenosis in the left and right carotid arteries. A, DynAngio image 702 ms after labeling alongside the TOF maximum-intensity projection at the level of the circle of Willis. B, Time-series data for voxels in the left and right MCA branches (circles=right, squares=left). γ-Variate model fit is shown (line). rTTP (seconds; C) and amplitude (D; %) maps show hemodynamics. Bright posterior signal shows the sagittal sinus.

phase encoding, nor does it require that slices be perpendicular to the vessels of interest.

The purpose of this study was to determine whether ASL-based DynAngio could be used to characterize circle of Willis hemodynamics, as it provides the primary means of collateral blood supply in the brain. We collected data from control subjects and patients with carotid artery disease to test the hypotheses that DynAngio hemodynamic measures are capable of showing age and carotid steno-occlusive disease–related influences on intracranial arterial hemodynamics. In patients who underwent CEA, we tested pre- and postsurgery differences.

Methods

This study was conducted with ethics approval from the Oxfordshire Research Ethics Committee.

Carotid Artery Disease Cohort

Thirty-seven patients with confirmed carotid artery disease were recruited to participate in this study. Twenty-four of 37 patients underwent CEA and were recruited to the study consecutively. Magnetic resonance imaging (MRI) data were collected within the 24 hours leading up to CEA and within the 24 hours after CEA. The 24-hour post-CEA MRI corresponds to the time frame in which the hyperperfusion syndrome is likely to occur.[11] The remaining non-CEA carotid artery disease patients were recruited from the vascular surgery laboratory database. Mean patient age was 70±9 years (range, 47 to 85 years; 10 women). Carotid arteries were assessed by Doppler ultrasound and are provided here for demographic information only: 0% to 49% unilateral, 3; 50% to 69% unilateral, 6; 70% to 99% unilateral, and contralateral <50%, 11; 70% to 99% unilateral, and contralateral >50%, 11; unilateral occlusion and contralateral <50%, 2; and unilateral occlusion and contralateral >50%, 4.

Control Cohort

Seventeen participants with no history of symptomatic carotid artery disease were recruited as controls to investigate aging effects as part of other ongoing trials. Mean age was 63±12 years (range, 45 to 87 years; 7 women). Ten of the 17 control participants had a history of transient ischemic attack but no significant carotid or vertebrobasilar artery (VBA) disease.

Magnetic Resonance Imaging

MRI data were collected on a 3-T scanner (TIM Trio; Siemens, Erlangen, Germany) with a 12-channel head receiver coil. DynAngio data were centered at the level of the circle of Willis. Flow-weighted contrast was achieved with a flow-sensitive alternating inversion-recovery pulsed ASL technique.[12] Time-resolved images were obtained by using a low flip-angle look locker spoiled gradient echo readout.[9] Flow information comes from the pulsed ASL difference images by subtracting the tag condition, achieved by a nonselective radiofrequency inversion pulse, from the control condition, in which a slab-selective radiofrequency inversion is used (Figure 1A). Single-slab, 2-dimensional images were acquired with the following parameters: 1×1-mm voxels, 50-mm slab thickness, repetition time/echo time/inversion time=1500 ms/3.7 ms/78 ms, 3 segments, flip angle of 10°, 20 inflow phases, and inflow increments of 78 ms. Images were spatially smoothed by using a 1.5-mm, full-width, half-maximum kernel as part of the postprocessing. In the tag images, a nonselective inversion pulse was used. In the control images, a slab-selective inversion thickness of 60 mm was used, compared with the 50-mm imaging slab. Therefore, the inflow blood water signal would come from water spins that are 5 mm above or below the image plane. The scan duration was 2 minutes, 42 seconds (see online-only Figure). Additional MRI consisted of the following: (1) a 3-plane localizer scan; (2) diffusion-weighted imaging (repetition time/echo time=4436 ms/93 ms, b-values=0, 1000 s/mm^2, 27 slices, and voxel dimensions of 1.6×1.6×3.0 mm^3); (3) gadolinium contrast-enhanced TOF angiography (field of view=200 mm, 1.1×0.8×1.0-mm^3 voxels, 40 slices per slab, 4 slabs, 6/8th partial Fourier k-space coverage, GRAPPA acceleration factor=2, repetition time/echo time=22 ms/4.08 ms, and scan duration=2:21). Maximum-intensity projection images were reconstructed from the TOF images at equivalent thickness to the DynAngio to facilitate comparison (Figure 1A) with the use of Osirix open-source software.[13] TOF images were used to characterize the anterior and posterior communicating arteries at the circle of Willis.

Dynamic Angiography Analysis

A γ-variate model was used to characterize the DynAngio data in terms of relevant hemodynamic parameters. The model was fit to the

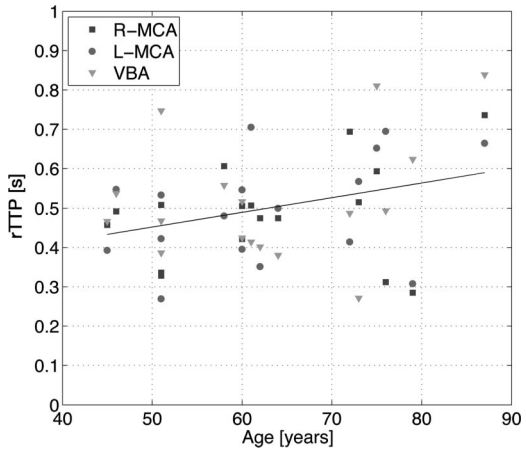

Figure 2. Mean DynAngio rTTP plotted as a function of age from controls (n=17). Data for the 3 arterial segments are labeled differently. Overall, there is an increasing rTTP trend with age that is significant (r^2=0.11, P<0.02).

DynAngio time-resolved signal in each voxel, based on the following expression (Figure 1B)[14]:

$$S(t)=\frac{A}{rTTP^{sh\cdot rTTP}}\cdot(t-t_0)^{sh\cdot rTTP}\cdot\exp(-sh\cdot((t-t_0)-rTTP))$$

The model parameters to be estimated were bolus arrival time (t_0, seconds), relative time to peak (rTTP, seconds; Figure 1C), amplitude (Figure 1D), relative amplitude (A, %; Figure 1C), and sharpness (sh, inverse seconds) for $t > t_0$. Initial model estimates (upper and lower bounds) were as follows: t_0=0.1 (0.28 to 2.26 seconds), rTTP=0.7 seconds (0 to 1.48 seconds), A=30% (0% to 400%), and sh=3 seconds^{-1} (0 to 8 seconds^{-1}). Amplitude was expressed as a fraction by dividing the peak signal in the sagittal sinus. This step facilitates intrasession and interparticipant comparison. rTTP is the time from t_0 to peak flow enhancement and is a measure of the slope from inflowing blood. The rTTP metric is chosen because it is independent of the bolus arrival time, will be less sensitive to timing delays and/or slice prescription, and matches the rTTP described by Ostergaard[15] for dynamic susceptibility contrast MRI. Model fitting was performed with the use of in-house Matlab code (Mathworks, Natick, MA). The number of estimated voxels was reported by arterial segment, based on the rTTP model-fit parameter. A voxel was significant when the ratio of the rTTP estimate divided by the fit standard deviation was >1.96, so as to approximate a z statistic threshold that would produce a significant fit at P<0.05.

Region-of-interest (ROI) analysis was performed to investigate the rTTP and amplitude hemodynamic metrics. A 5×5-voxel ROI was placed manually at the inlet arterial segments of the right middle cerebral artery (MCA), left MCA, and VBA for each participant. Correlation and linear regression analysis were performed to determine the effect of age and internal carotid artery (ICA) stenosis on rTTP (SPSS for Macintosh, version 17.0; SPSS, Chicago, IL). Paired 2-tailed t tests were performed to compare pre- and post-CEA data.

Results

DynAngio in the Control Cohort

Mean rTTP increased significantly with age, when all arterial segments were considered, according the following expression: rTTP=0.266+0.004×age, which corresponds to an increase of 40 ms per decade (Figure 2; P<0.02). The number of voxels tended to decrease with age, but this decrease was significant in the VBA segment only (P<0.03).

Cohort Comparison

Patients were significantly older than controls, with a mean age of 70±9 years compared with controls who were 63±12 years (P<0.03). Fewer rTTP voxels were found in the right MCA and left MCA segments for patients compared with controls (P<0.006), but no significant difference was found for the VBA segment (P>0.93).

DynAngio in the Patient Cohort

Mean rTTP increased significantly with the percent ICA stenosis in a linear-regression model that included age and ICA stenosis as independent variables (P<0.05). For the CEA patients, only pre-CEA data were included. Pre- versus post-CEA differences are shown in the rTTP maps for 2 patients (Figures 3 and 4). Figure 5 shows the ROI analysis for rTTP data before and after CEA. rTTP in the MCA branch ipsilateral to the CEA decreased significantly, from 564±171 ms before CEA to 471±119 ms after CEA (2-tailed paired t test: t=2.58, df=21, P<0.017). rTTP values did not change significantly in the contralateral MCA or VBA ROIs (P>0.49).

Ipsilateral MCA amplitude increased significantly, from 41±25.7% before CEA to 55±24.1% after CEA (Figure 6; 2-tailed paired t test: t=2.87, df=22, P<0.009). Patients with an intact circle of Willis (13 patients) showed larger increases in amplitude before versus after CEA compared with patients with at least 1 communicating artery missing (9 patients; ANOVA F=4.5, P=0.045). Contralateral MCA and VBA ROIs showed no significant amplitude change.

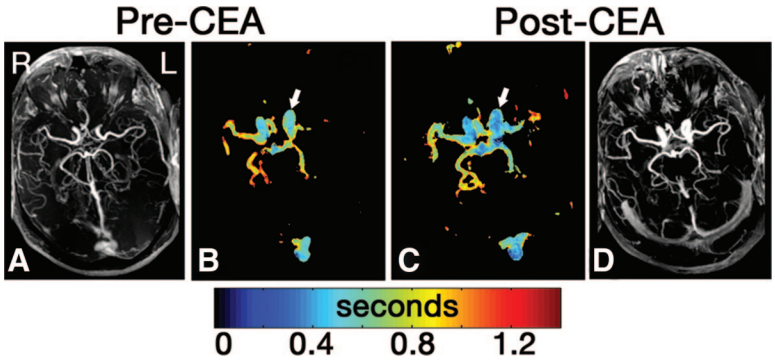

Figure 3. Maximum-intensity projection TOF (A and D) and DynAngio rTTP (B and C) for patient 1 with a right ICA stenosis of 30% and a left ICA stenosis of 85% who underwent left CEA. A decrease in rTTP after CEA is shown at the left carotid siphon (arrows).

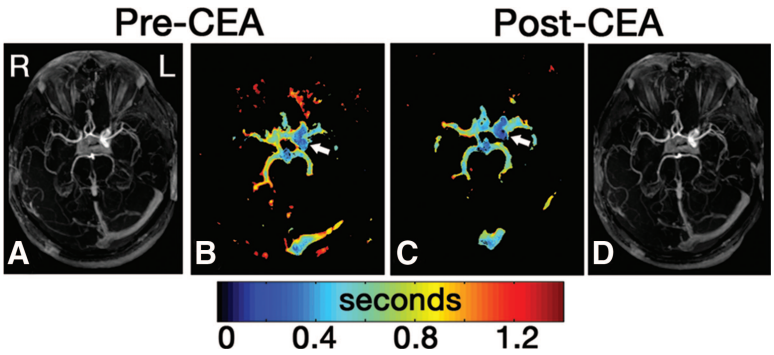

Figure 4. Maximum-intensity projection TOF (A and D) and DynAngio rTTP (B and C) for patient 2 with a right ICA stenosis of 100% and a left ICA stenosis of 65% who underwent left CEA. Arrows indicate the left carotid siphon where rTTP was reduced after CEA.

Discussion

This study demonstrates the utility of ASL-based, time-resolved angiography for the characterization of intracranial hemodynamics. There are 3 novel findings: (1) rTTP increased with age among controls, (2) rTTP increased with the degree of extracranial ICA stenosis, and (3) rTTP decreased and amplitude increased in the MCA segment ipsilateral to the surgery at 1 day after CEA compared with before CEA. Results from the patients with carotid artery disease illustrate the clinical potential of this DynAngio technique and extend the work by others.[9,10]

Among controls, rTTP in the MCA increased with age. The rTTP metric is related to the slope of the bolus inflow and is likely influenced by flow velocity, vessel diameter, and tortuosity, which is related to pathologic aging processes.[16] Characterization of aging effects in controls has not previously been reported with this ASL-based technique. Others have used alternative modalities to show that vascular compliance decreases and that common carotid artery stiffness increases with age.[17,18] Cardiac gating was not performed in this study, so our hemodynamic metrics were averaged over the cardiac cycle. Future work could address cardiac effects on this DynAngio because this is an area in the literature that is developing.[19,20] We found significant differences between patients and controls, such as the number of detected voxels in the right and left MCAs. Differences in vascular anatomy and the fact that the cohorts were not equally matched for age and sex may have influenced the results.

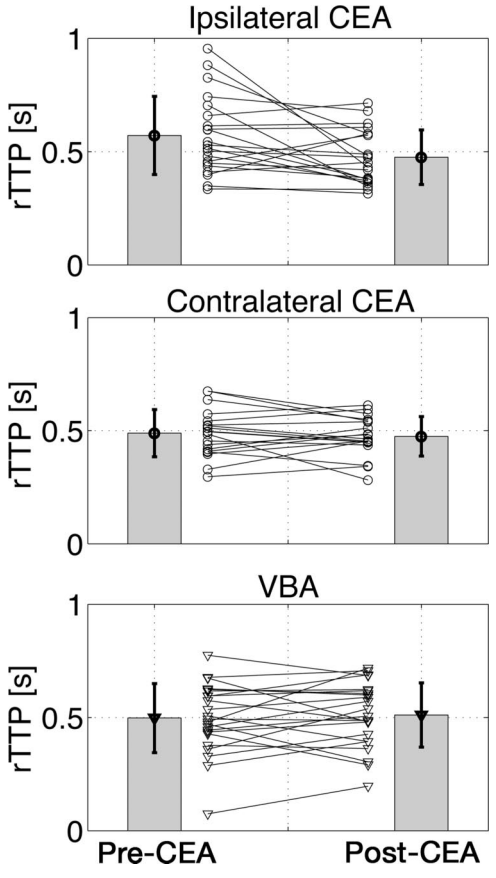

Figure 5. DynAngio rTTP for patients who underwent CEA. A 2-tailed paired *t* test showed that post-CEA rTTP was significantly reduced compared with pre-CEA rTTP in the MCA ipsilateral to the CEA ($P<0.017$) but not for the contralateral MCA or VBA. Each line represents data from 1 patient (left=before CEA, right=after CEA).

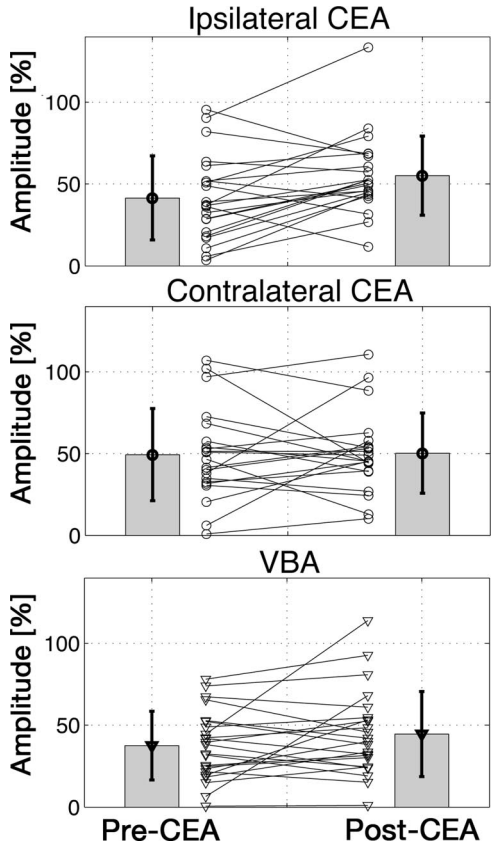

Figure 6. DynAngio amplitude increased significantly after CEA in the ipsilateral MCA compared with before CEA ($P<0.009$) but not for the contralateral MCA or VBA ROIs. Each line represents data from 1 patient (left=before CEA, right=after CEA).

Our second finding was that rTTP values increased significantly with ICA stenosis, which illustrates that it is possible to quantify the effect of extracranial stenosis on distal intracranial arteries. Fifteen of a possible 74 MCA ROIs were not included, however, for 1 of the following reasons: (1) the MCA segment showed an insufficient number of voxels to place an ROI, (2) image quality was poor owing to head motion, or (3) a significant bolus delay affected the estimates, such as t_0 or rTTP. With respect to the latter, further work is required to determine how best to schedule the inflow measurements. This might be accomplished by preceding the DynAngio sequence with a phase-contrast MRA, for example, to calculate velocity profiles.

The final results pertain to the significant CEA-related changes that were observed. rTTP decreased significantly after CEA, which could argue for an improved flow profile downstream. Amplitude increased significantly after CEA, which is consistent with previous ICA flow changes.[11] Post-CEA data were obtained 24 hours after surgery, before the patients being discharged, which is not a steady-state period but is important in terms of the hyperperfusion syndrome.[11] The DynAngio scan duration was short and does not require injected contrast material; therefore, it would lend itself well to longitudinal monitoring.

Hemodynamic modeling used 20 inflow time points to extract the metrics, producing a temporal precision that was greater than the 78-ms sampling interval. The pulsed ASL technique was not spatially selective for a particular arterial supply and has the advantage of labeling a large volume of arterial blood water. However, there are 2 limitations of the current method. First, the single imaging slab has limited brain coverage, although 3-dimensional dynamic MRA sequences are being developed.[21,22] Second, the nonselective labeling included venous blood water. The venous ASL signal was principally from the sagittal sinus and was used to normalize arterial amplitude values.

Chronic hypoperfusion and hemodynamic impairment are important factors in cerebrovascular diseases such as stroke[23,24] and transient ischemic attack.[25–27] The current study demonstrates that it is possible to characterize intracranial arterial hemodynamics along the length of an arterial segment in a time-efficient manner. Others have shown that significant hemodynamic effects exist in patients with carotid occlusive disease in their ipsilateral cerebral hemisphere.[28] We have recently reported hemispheric asymmetry in the arterial cerebral blood volume of patients with severe stenoses by using a noninvasive MR technique.[29] Ultimately, dynamic MRA sequences may be useful in explaining downstream perfusion and in identifying patients who will most benefit from surgical intervention.

Acknowledgments

We acknowledge the Heart and Stroke Foundation of Canada (B.J.M.), the Medical Research Council (P.J.), the Dunhill Medical Trust (P.J., M.J.D.), and the German Ministry of Education and Research (M.G.).

Source of Funding

This study was supported by the NIHR Oxford Biomedical Research Centre.

Disclosures

None.

References

1. Derdeyn CP, Yundt KD, Videen TO, Carpenter DA, Grubb RL Jr, Powers WJ. Increased oxygen extraction fraction is associated with prior ischemic events in patients with carotid occlusion. *Stroke*. 1998;29:754–758.
2. Barnett HJ, Taylor DW, Eliasziw M, Fox AJ, Ferguson GG, Haynes RB, Rankin RN, Clagett GP, Hachinski VC, Sackett DL, Thorpe KE, Meldrum HE, Spence JD. Benefit of carotid endarterectomy in patients with symptomatic moderate or severe stenosis. North American Symptomatic Carotid Endarterectomy Trial Collaborators. *N Engl J Med*. 1998;339:1415–1425.
3. Wolf O, Heider P, Heinz M, Poppert H, Schmidt-Thieme T, Sander D, Grafin von Einsiedel H, Brandl R. Frequency, clinical significance and course of cerebral ischemic events after carotid endarterectomy evaluated by serial diffusion weighted imaging. *Eur J Vasc Endovasc Surg*. 2004; 27:167–171.
4. Muller M, Reiche W, Langenscheidt P, Hassfeld J, Hagen T. Ischemia after carotid endarterectomy: comparison between transcranial Doppler sonography and diffusion-weighted MR imaging. *AJNR Am J Neuroradiol*. 2000;21:47–54.
5. Hendrikse J, Rutgers DR, Klijn CJ, Eikelboom BC, van der Grond J. Effect of carotid endarterectomy on primary collateral blood flow in patients with severe carotid artery lesions. *Stroke*. 2003;34:1650–1654.
6. Korosec FR, Frayne R, Grist TM, Mistretta CA. Time-resolved contrast-enhanced 3D MR angiography. *Magn Reson Med*. 1996;36:345–351.
7. Gunther M, Bock M, Schad LR. Arterial spin labeling in combination with a look-locker sampling strategy: inflow turbo-sampling EPI-FAIR (ITS-FAIR). *Magn Reson Med*. 2001;46:974–984.
8. Williams DS, Detre JA, Leigh JS, Koretsky AP. Magnetic resonance imaging of perfusion using spin inversion of arterial water. *Proc Natl Acad Sci U S A*. 1992;89:212–216.
9. Sallustio F, Kern R, Gunther M, Szabo K, Griebe M, Meairs S, Hennerici M, Gass A. Assessment of intracranial collateral flow by using dynamic arterial spin labeling MRA and transcranial color-coded duplex ultrasound. *Stroke*. 2008;39:1894–1897.
10. van Osch MJ, Hendrikse J, Golay X, Bakker CJ, van der Grond J. Non-invasive visualization of collateral blood flow patterns of the circle of Willis by dynamic MR angiography. *Med Image Anal*. 2006;10:59–70.
11. Hosoda K, Kawaguchi T, Shibata Y, Kamei M, Kidoguchi K, Koyama J, Fujita S, Tamaki N. Cerebral vasoreactivity and internal carotid artery flow help to identify patients at risk for hyperperfusion after carotid endarterectomy. *Stroke*. 2001;32:1567–1573.
12. Kim SG. Quantification of relative cerebral blood flow change by flow-sensitive alternating inversion recovery (FAIR) technique: application to functional mapping. *Magn Reson Med*. 1995;34:293–301.
13. Rosset A, Spadola L, Ratib O. Osirix: an open-source software for navigating in multidimensional dicom images. *J Digit Imaging*. 2004;17: 205–216.
14. Rausch M, Scheffler K, Rudin M, Radu EW. Analysis of input functions from different arterial branches with γ-variate functions and cluster analysis for quantitative blood volume measurements. *Magn Reson Imaging*. 2000;18:1235–1243.
15. Ostergaard L. Principles of cerebral perfusion imaging by bolus tracking. *J Magn Reson Imaging*. 2005;22:710–717.
16. D'Esposito M, Deouell LY, Gazzaley A. Alterations in the bold fMRI signal with ageing and disease: a challenge for neuroimaging. *Nat Rev Neurosci*. 2003;4:863–872.
17. Hansen F, Mangell P, Sonesson B, Lanne T. Diameter and compliance in the human common carotid artery–variations with age and sex. *Ultrasound Med Biol*. 1995;21:1–9.
18. Vermeersch SJ, Rietzschel ER, De Buyzere ML, De Bacquer D, De Backer G, Van Bortel LM, Gillebert TC, Verdonck PR, Segers P. Age and gender related patterns in carotid-femoral PWV and carotid and femoral stiffness in a large healthy, middle-aged population. *J Hypertens*. 2008; 26:1411–1419.
19. Wu WC, Mazaheri Y, Wong EC. The effects of flow dispersion and cardiac pulsation in arterial spin labeling. *IEEE Trans Med Imaging*. 2007;26:84–92.
20. Gallichan D, Jezzard P. Modeling the effects of dispersion and pulsatility of blood flow in pulsed arterial spin labeling. *Magn Reson Med*. 2008; 60:53–63.

21. Hori M, Shiraga N, Watanabe Y, Aoki S, Isono S, Yui M, Ohtomo K, Araki T. Time-resolved three-dimensional magnetic resonance digital subtraction angiography without contrast material in the brain: initial investigation. *J Magn Reson Imaging*. 2009;30:214–218.
22. Guenther M, Warmuth C, Schad LR. Non-invasive dynamic 3D angiography with its-3D-FAIR. Proceedings from the ISMRM 10th Scientific Meeting. 2001:1565.
23. Chalela JA, Alsop DC, Gonzalez-Atavales JB, Maldjian JA, Kasner SE, Detre JA. Magnetic resonance perfusion imaging in acute ischemic stroke using continuous arterial spin labeling. *Stroke*. 2000;31:680–687.
24. Siewert B, Schlaug G, Edelman RR, Warach S. Comparison of epistar and T2*-weighted gadolinium-enhanced perfusion imaging in patients with acute cerebral ischemia. *Neurology*. 1997;48:673–679.
25. Bokkers RP, van der Worp HB, Mali WP, Hendrikse J. Noninvasive MR imaging of cerebral perfusion in patients with a carotid artery stenosis. *Neurology*. 2009;73:869–875.
26. MacIntosh BJ, Lindsay AC, Kylintireas I, Kuker W, Gunther M, Robson MD, Kennedy J, Choudhury RP, Jezzard P. Multiple inflow pulsed arterial spin-labeling reveals delays in the arterial arrival time in minor stroke and transient ischemic attack. *AJNR Am J Neuroradiol*. 2010;31:1892–1894.
27. Derdeyn CP, Grubb RL Jr, Powers WJ. Cerebral hemodynamic impairment: methods of measurement and association with stroke risk. *Neurology*. 1999;53:251–259.
28. Hendrikse J, van Osch MJ, Rutgers DR, Bakker CJ, Kappelle LJ, Golay X, van der Grond J. Internal carotid artery occlusion assessed at pulsed arterial spin-labeling perfusion MR imaging at multiple delay times. *Radiology*. 2004;233:899–904.
29. Donahue MJ, Sideso E, MacIntosh BJ, Kennedy J, Handa A, Jezzard P. Absolute arterial cerebral blood volume quantification using inflow vascular-space-occupancy with dynamic subtraction magnetic resonance imaging. *J Cereb Blood Flow Metab*. 2010;30:1329–1342.